

Article

Design of Unmanned Road Widths in Open-Pit Mines Based on Offset Reaction Times

Liu Han and Peng Liu * 

School of Mines, China University of Mining and Technology, Xuzhou 221116, China; hanliucumt@163.com

* Correspondence: ts22020038a31tm@cumt.edu.cn

Abstract: In an effort to enhance the efficiency and safety of open-pit mines, this study explores the optimization of end slope road parameters and slope structures, specifically focusing on unmanned driving lanes. A significant aspect of the study is the development of a truck trajectory offset model, which considers the different reaction times between automated sensors and human drivers in adapting to environmental changes. To test these concepts, the study uses numerical simulations to confirm the stability of the proposed end slope designs. Using Victory West Mine No. 1 as a case study, the research determines the optimized width for unmanned driving lanes and the maximum angle for the safe steepening of end slopes. The findings indicate that the optimized unmanned lane width for NTE240 mining dump trucks is 1743 mm, allowing for a 2-degree increase in the slope angle at the south end slope. This optimization leads to a steep mining stripping volume of 3.2735 million m³ and a coal output of 2.49628 million tons, maintaining a stripping ratio of 1.31 m³/t. These results demonstrate that unmanned driving road width optimization not only ensures slope safety but also significantly boosts the economic benefits of steep mining in open-pit mines.

Keywords: unmanned driving; truck dynamics; offset reaction time; road width; economic benefits



Citation: Han, L.; Liu, P. Design of Unmanned Road Widths in Open-Pit Mines Based on Offset Reaction Times. *Appl. Sci.* **2024**, *14*, 2995. <https://doi.org/10.3390/app14072995>

Academic Editor: Mónica Calero de Hoces

Received: 4 March 2024

Revised: 27 March 2024

Accepted: 29 March 2024

Published: 2 April 2024



Copyright: © 2024 by the authors. Licensee MDPI, Basel, Switzerland. This article is an open access article distributed under the terms and conditions of the Creative Commons Attribution (CC BY) license (<https://creativecommons.org/licenses/by/4.0/>).

1. Introduction

In recent years, the focus for open-pit mines has been on advancing their technological capabilities and integrating information technology with industrialization processes. Mine intelligence, unmanned technology, and eco-friendliness are key areas of energy technology innovation supported by the state [1]. In this process, unmanned technology as a high-tech solution has been extensively implemented in open-pit mines. The implementation of autonomous technologies in surface mine transportation can effectively mitigate issues such as low production efficiency, elevated safety hazard, and increased coal compression levels caused by traditional transportation practices. Komatsu Company's autonomous mining dump trucks have been operational for several years in Australia, Chile, and other countries, amassing ample experience. Meanwhile, China's autonomous mining truck technology has yet to progress beyond the developmental stage [2].

In recent years, several of China's major open-pit mines have introduced autonomous vehicles, including the State Energy Nortel Shengli Energy Shengli West No. 1 Open-Pit Coal Mine, the State Energy Group Baorixil Open-Pit Coal Mine, and the Huaneng Yimin Coal and Power Limited Liability Company's Yimin Open-Pit Coal Mine [3,4]. Regarding technical models of unmanned mining dump trucks, despite significant contributions from scholars both domestically and internationally in areas such as truck scheduling [5], trajectory tracking [6], and attitude control [7], there has been little research conducted on the width of unmanned lanes in surface mines. Due to their precise sensing and localization abilities [8], unmanned vehicles have shorter perception times and stronger reaction capabilities than human drivers. This necessitates the reevaluation of traditional road designs, as they may not meet the width requirements necessary for unmanned vehicles. For open-pit mining, reducing the width of the flat disk and increasing the slope

angle can result in significant economic benefits with the implementation of end-slope mining. However, there is also a certain risk to slope safety, and protecting the slope stability is a prerequisite for applying the end-slope mining method [9]. For open-pit mines that have been put into production, the surface boundary is fixed, the upper step of the slope remains unchanged when an optimization process is carried out, and the lower step is pushed outward to optimize the slope angle for end-slope mining. For new intelligent mines, the bottom boundary can be taken as the boundary, through optimizing the width of the transportation road and increasing the slope angle of the end slope, to reduce the area of land acquisition and reduce the damage to the land excavation machinery.

This paper optimizes open-pit mine transportation road width designs under unmanned conditions. We analyze differences between manned and unmanned roads in open-pit mines to provide a basis for improved transportation efficiency and safety. An in-depth study of unmanned road widths is conducted. Reducing the width of the transportation flat pan can lead to an improvement in the slope angle and can decrease the average stripping ratio. Therefore, optimizing the road width using unmanned technology while ensuring slope safety can result in significant economic benefits. This is a crucial technology for constructing intelligent open-pit mines.

2. Methodology

2.1. Open-Pit Mine Road Width Analysis

As shown in Figure 1, an open-pit mine roadway consists of a traveled way, a retaining wall, a protective area, and a safety width [10].

- (1) Travel lanes: The two-lane design includes two mine truck haul roads, which can ensure that two haul trucks pass at the same time, while the single-lane design has only one mine truck haul road.
- (2) Retaining walls: A mound of loose stripped material with a profile pattern that is roughly an isosceles trapezoidal shape with a natural buildup.
- (3) Protected area: An area that is artificially delineated and located near the inside of a hauling pan to prevent falling rocks from impacting personnel and equipment and causing safety accidents, which is generally closed to traffic.
- (4) Lateral safety distance: The main categories are the safe width for trucks meeting on two-lane type transport roads, the safe width between trucks and retaining walls and the width of the protection zone.

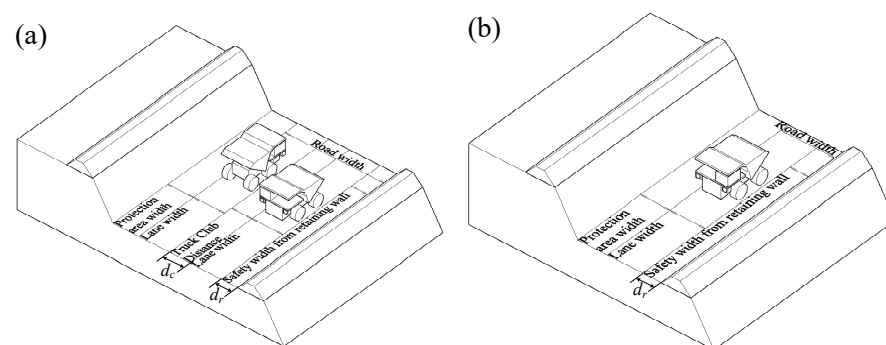


Figure 1. Open-pit end wall road: (a) two-lane road; (b) single-lane road.

In the establishment of road widths for open-pit mines, one must consider the maximum widths of the diverse types of mining trucks utilized in the mine, the minimum lateral safety distance when two mining trucks intersect, and the safe width of the mining trucks in relation to the road's edge. Equation (1) displays the conventional road width [11]:

$$W = 2l + d_c + 2d_r \quad (1)$$

where W is the width of the road in m, l is the width of the largest type of mine truck used in the open-pit mine in m, d_c indicates the meeting distance of two mine trucks in m, and d_r indicates the distance between the trucks and the edge of the road, which shall not be less than 5 m for the non-working slope and shall not be less than 4 m for the working slope.

2.2. Unmanned Road Analysis

The current guidelines are unsuitable for the changing needs of future smart open-pit mining and hybrid settings where unmanned and manned vehicles operate, due to the differences in operational models between unmanned and manned driving scenarios. Consequently, there is a need to reassess the current road design guidelines for open-pit mines. Unmanned vehicle networking, remote monitoring, and sensor technologies [12] have revolutionized the traditional driving mode, which relies on human perceptions of the environment. This has reduced the time the vehicle interacts with the environment, increasing its speed. Consequently, this affects the standard for the design speed of open-pit mine trucks [13].

Unmanned vehicles no longer rely on human manipulation. The current unmanned environmental sensing [14], vehicle positioning [15], vehicle scheduling [16], behavioral decision-making [17], and computer control systems form the entire system, which can simulate or even exceed the driver's method of controlling the vehicle [18]. If we reduce the instability and diversity of the driver's control of the vehicle, this can decrease the width requirements for open-pit mine transportation roads. The path decision-making process for unmanned vehicle driving is completed by the control system. When all vehicles are networked, the system will analyze their destinations and road conditions to plan the best driving route. This greatly improves the waiting times for mining trucks stopping at mining and loading points and enhances the overall operational efficiency of the road network [19].

Unmanned driving commonly denotes the technology or system enabling a vehicle to function autonomously. The system comprises an amalgamation of sensors, cameras, AI systems, and additional technologies enabling the vehicle's navigation and reaction to its surroundings.

The primary distinction between unmanned and manned (traditional) driving lies in how humans manage the vehicle.

During crewed driving, a person takes charge of the vehicle, handling all navigational, speed, and traffic response decisions. Conversely, during autonomous driving, the choices are determined by the vehicle's internal computer configurations, relying on sensor data and preset algorithms.

It is essential for human drivers to stay persistently alert to the streets and their environment. Autonomous vehicles depend on ongoing monitoring from sensors and cameras to stay informed about their surroundings, theoretically decreasing the likelihood of incidents related to distractions.

The reaction time of human drivers is subject to influence from multiple elements such as tiredness, diversions, and disability. Unmanned vehicles are likely to respond more quickly to unexpected events owing to their sensors' ability to identify and interpret information more rapidly than humans.

The advantages and disadvantages of unmanned vehicles relevant to this study are summarized in Table 1.

Table 1. Advantages and disadvantages of unmanned vehicles.

Advantages	Disadvantages
No blind spots, more accurate judgement of distances	Highly affected by bad weather and complicated road conditions
Faster and more accurate responses to unexpected situations	Cannot understand some of the potential rules of the road, such as accelerating or decelerating as quickly as possible to avoid parallel driving
Never get tired and work more efficiently	

Based on a prior analysis of the width of the road of an open-pit mine’s end slope, the traditional open-pit mine road was given a larger road width and safety distance to mitigate safety accidents caused by the mining area’s unique environment, operational driver errors, driver fatigue, vehicle failure, vehicle aging, and other related issues during the production and transportation processes. The width of the road at the end of an open-pit mine is affected by four main factors, namely humans, vehicles, the road itself, and the environment. However, unmanned mine trucks are not driven by a human driver; instead, they are controlled by a variety of vehicle-mounted sensors and sensors on both sides of the road in the open-pit mine. These sensors detect vehicle information and provide feedback to the control system in order to control the vehicle.

Therefore, studies of unmanned lane widths in open-pit mines only need to consider the equipment parameters of unmanned mining trucks and the safe road width, without taking personnel influence into account.

2.3. Optimization of Road Width

The sensor detects information when the vehicle is deviated and then transmits it to the processing center. The center subsequently sends instructions to the controller, which takes about 0.4 s to control the truck’s response. In comparison, a human typically takes about 1.2 s after observing an obstacle and making a judgement [20]. As presented in Figure 2, the width of the unmanned road that is optimal can be calculated using Equation (2) based on the maximum distance of the mining dump truck’s lateral offset during the sensor reaction phase (x_{max}) and the maximum distance of the truck’s lateral offset during the driver reaction phase (x'_{max}).

$$x_{op} = x'_{max} - x_{max} \tag{2}$$

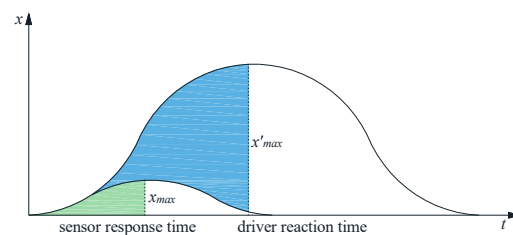


Figure 2. Lateral offset back to positive curve.

To obtain precise transverse offset distance measurements for mining dump trucks, it is imperative to create a compliant transverse dynamics model for these vehicles and investigate the transverse forces acting on them while steering. Due to the intricate nature of these forces, a single truck model was designed to characterize the transverse dynamics of mining dump trucks in order to simplify the algorithm. As a result, the transverse and longitudinal aerodynamic effects were overlooked.

From the lateral dynamics model of the vehicle shown in Figure 3, it is evident that the equations of motion for the vehicle’s lateral movement can be derived.

$$F_{xf} \cos \theta + F_{xb} = m(\dot{v}_x + v_y r) \tag{3}$$

where F_{xf} and F_{xb} represent the lateral deflection forces of the front and rear wheels, respectively; θ denotes the angle of rotation of the front wheel; m signifies the mass of the vehicle; v_x indicates the lateral speed of the vehicle; v_y represents the longitudinal speed; and r is the transverse angular velocity.

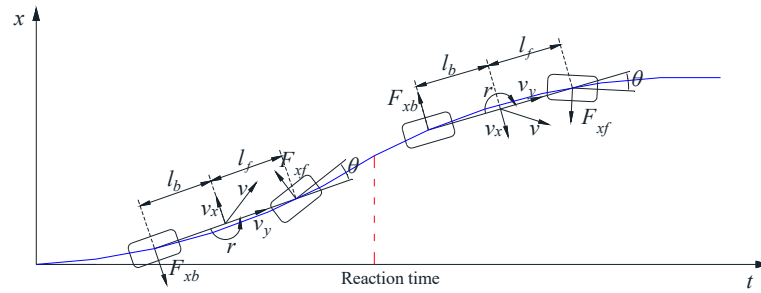


Figure 3. Lateral dynamics model.

The theory of the brush tire model suggests that there exists a linear relationship between the tire’s side deflection force and the side deflection angle when the latter is less than 5°.

$$F_{xf}, F_{xb} = \begin{cases} -C_{\alpha} \tan \alpha + \frac{C_{\alpha}^2}{3\mu F_z} |\tan \alpha| \tan \alpha - \frac{C_{\alpha}^3}{27\mu F_z} \tan^3 \alpha, & |\alpha| < \arctan\left(\frac{3\mu F_z}{C_{\alpha}}\right) \\ -\mu F_z \operatorname{sgn} \alpha, & |\alpha| \geq \arctan\left(\frac{3\mu F_z}{C_{\alpha}}\right) \end{cases} \quad (4)$$

where the vehicle tire’s lateral deflection stiffness (C_{α}), the wheel’s lateral deflection angle (α), the road surface adhesion coefficient (μ), and the tire’s vertical force (F_z) are all important factors to consider.

When the lateral deflection angle and slip rate of the tire are low, the resulting lateral force on the tire is proportional to the lateral deflection stiffness. Therefore, it is possible to express F_{xf} and F_{xb} in Equation (4) using Equation (5):

$$F_{xf}, F_{xb} = C_{\alpha} \times \alpha \quad (5)$$

If the distance from the front wheel of the truck to the center of gravity is known, as well as the vertical force F_t of the truck’s tires, the truck’s moment of inertia M can be calculated as follows:

$$M_f = l \times F \quad (6)$$

The relationship between the rotational moment M and the angular acceleration β can be described as follows:

$$M = J \times \beta \quad (7)$$

where the truck’s moment of inertia is $J = 5757 \text{ kg/m}^3$.

The angular acceleration β is determined by the following equation:

$$\beta = \frac{d\omega}{dt} \quad (8)$$

$$x = \sum_{i=1}^{n-1} 2v \cdot dt \cdot \tan\left(i \cdot \omega dt \cdot \frac{\pi}{180}\right) + v \cdot dt \cdot \tan\left(n \cdot \omega dt \cdot \frac{\pi}{180}\right) \quad n = t/dt \quad (9)$$

Based on the instantaneous turning angle ω , the sensor response time t_s , and the driver response time t_d , we can calculate the maximum distance x of the truck’s lateral deflection.

2.4. End-Slope Mining Method

A significant amount of resources in the lower part of the end slope cannot be extracted, leading to a decrease in the resource recovery rate and the economic benefit of the mine. Increasing the angle of the end slope can significantly increase the amount of resources recovered from the overburden, although it also increases the pressure on the safety of the end slope. Therefore, to achieve the maximum resource recovery rate and mine economic benefits, the angle of the end slope must be optimized while ensuring overall safety and stability of the slope.

Figure 4 illustrates the end-slope mining method, which increases the end gang angle from β to α by increasing the bench angle and reducing the width of the bench floor. This allows for the extraction of coal resources in the BCED area while also increasing the amount of earth stripping in the ABC area. The stripping ratio for end-slope mining is very small, resulting in better economic benefits. Our research on unmanned road widths has shown that reducing it can significantly decrease the size of the bench floor. Additionally, the implementation of end-slope mining technology can result in substantial economic benefits.

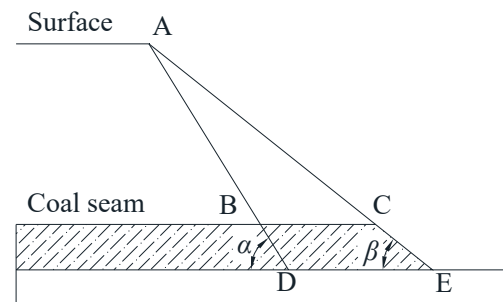


Figure 4. End-slope mining method. A denotes the top of the slope, B denotes the upper edge of the coal seam behind the end-slope mining, C denotes the upper edge of the present coal seam, D denotes the bottom of the side slope behind the end-slope mining, and E denotes the bottom of the present slope.

3. Case study and Results

3.1. Analysis of the Return Distance for Lateral Offset of Mining Trucks

This paper presents a description of a driverless truck that has been converted from an NTE240 mining dump truck, which is employed in the Shengli West No. 1 open-pit coal mine of Guoneng Beidian Shengli Energy. A lateral dynamics model of the NTE240 mining dump truck was established, with the relevant parameters presented in Table 2.

Table 2. Technical parameters of the NTE240 mining truck.

Description	Value
Rated load capacity	220~236 t
Loading volume	114 m ³
Maximum speed	64 km/h
Minimum turning radius	15.2 m
Loading height	6600 mm
Overall length	14,800 mm
Overall width	7640 mm
Total height	7300 mm
Unladen mass	150 t
Distance from the center of the front axle to the center of mass	3.27 m
Distance from center of the shaft to center of mass after no load	2.93 m

A truck tire model in Trucksim was used to determine the relationship between the tire droop force and the side deflection force of the truck's front wheel for a given angle of side deflection. The small wheel offset angle during regular straight line vehicle motion contrasts with the substantial vertical force the NTE240 mining dump truck's tire endures when supporting its own weight. Figure 5 demonstrates the truck's deflection during typical driving, with the vehicle's side deflection forces ranging from 200 kN to 350 kN.

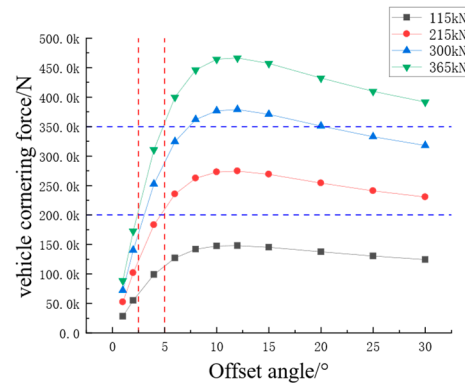


Figure 5. Tire model made using Trucksim.

From Table 1, it is clear that the center of gravity of the truck is 3.27 m from the center of the front axle when unladen, and the moment of the front wheels is also known.

The maximum distance x_{max} of the lateral offset of the mining dump truck during the sensor reaction phase and the maximum distance x'_{max} of the lateral offset of the truck during the driver reaction phase can be determined as $x'_{max} = 1960$ mm and $x_{max} = 217$ mm, respectively. According to Equation (2), the width of the road of the unilateral transport flat plate of the autonomous vehicle, which can be optimized for reduction, can be calculated as $x_{op} = x'_{max} - x_{max} = 1743$ mm.

3.2. Economic Benefits of Unmanned Road Building

This case study examines the Shengli West No. 1 Surface Coal Mine, situated 5 km north of Xilinhot City, Xilingol League, Inner Mongolia Autonomous Region. The coal seams in this surface mine have a dip angle of less than 5° and the primary seams are the No. 5 and No. 6 coal seams. The No. 5 seam has an average recoverable thickness. The first mining area hosts the No. 5 and No. 6 coal seams, with average thicknesses of 15.6 m and 32.23 m, respectively, while the latter is 31.4 m in the same area. A total of 13 stripping steps and 5 mining steps are present, with the heights of the stripping steps being 15 m and 10 m. All findings are based on the extraction of the non-grainy coal seams. The No. 6 coal seam in the initial mining region has an average thickness of 32.23 m, while the average thickness of the No. 6 coal seam in the same area is 31.4 m. The height of the stripping steps here stands at 15 m, whereas the coal mining steps have heights of 10 m and 15 m. Presently, there are 13 stripping steps and 5 coal mining steps. The transport equipment available for use mainly includes 91 t, 108 t, and 220 t mining dump trucks, with over 50,220 t dump trucks being operational. Figure 6 shows a 3d diagram of the Shengli open pit mine.

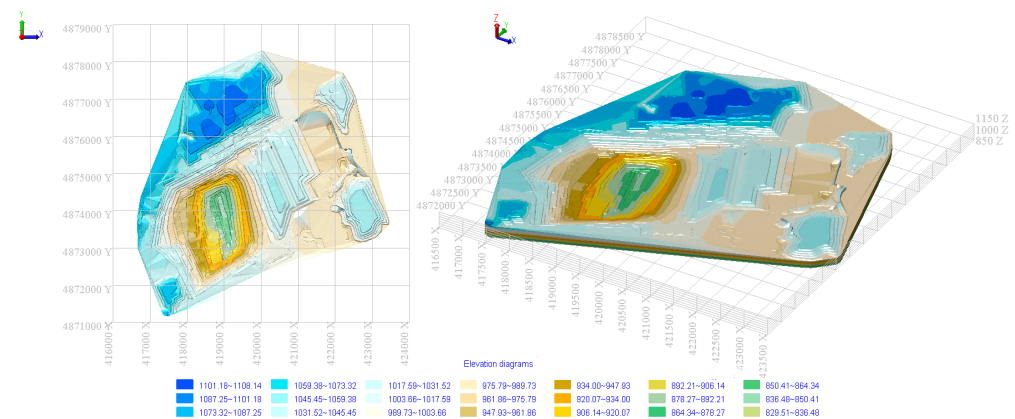


Figure 6. A 3D diagram of the Shengli West No. 1 Open-Pit Mine.

The previously calculated x_{op} only represents the optimized width of a single lane and a single side of the mining truck. Therefore, the optimized width of the road surface for dual vehicles is $x_d = 4x_{op} = 6.972$ m and the optimized width for single-vehicle road surfaces is $x_s = 2x_{op} = 3.486$ m. The average length of the southern slope at Shengli West No. 1 Open-Pit Coal Mine is 1000 m. The optimized transportation road width is utilized to determine the profile structure of the southern slope following lane compression according to the “Preliminary Design Specification for 2800 Mt/a Shengli Energy Shengli No. 1 Open-Pit Coal Mine” on the division of steps along the south slope road. As shown in Figure 7, after the optimization of the end slope road width, the stripping volume is 3,273,500 m³, the coal production volume is 2,496,280 t, and the stripping ratio to the slope is 1.31.

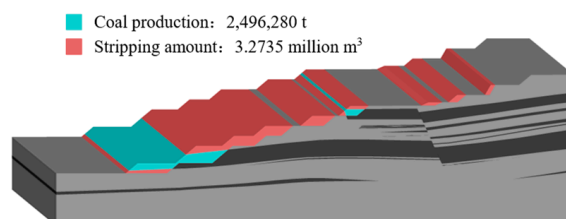


Figure 7. Road width optimization of the south end slope.

Based on the lithology of the Shengli West No. 1 Open-Pit Coal Mine’s stratum, we analyzed the stability of the south slope before and after optimization. Table 3 illustrates the physical and mechanical properties of the slope rock body during the stability analysis of the open-pit mine.

Table 3. Physical and mechanical parameters of the rock mass.

Rock Formation	Cohesion/kPa	Internal Friction Angle/°	Density/kN·m ⁻³
Quaternary	18	22~24	16.5
Mudstone	20	20~22	19.3
Siltstone	50	24~26	20.3
Coal	40	22~27	13.8
Mudstone with sandstone interbedded	20	20~23	20.0
Middle conglomerate	15	22~24	21.0
Siltstone mudstone	20	21~23	20.5

Based on the stratigraphic structure of the south slope and the principle of the limit equilibrium, a two-dimensional stability analysis method was employed to examine the landslide modelling of slopes. The resulting analysis showed the location of the potential sliding surface and the extent of the sliding body throughout the slope.

The stability of the south slope profile was analyzed using the Morgenstern method in conjunction with the slope stability analysis software SLOPE/W 11.4.0.18. The impact of mine dump truck loading on the slope stability was also taken into account to identify the most hazardous sliding surface of the south slope. The results of the slope stability analysis are presented in Figure 8.

Requirements for open pit mine slope stability coefficients [21], end slopes with a service life of less than 10 years must have a stability coefficient of at least 1.10. Figure 8 shows that both the original slope and optimized slope stability coefficients exceed the required specifications, indicating that the south slopes are stable.

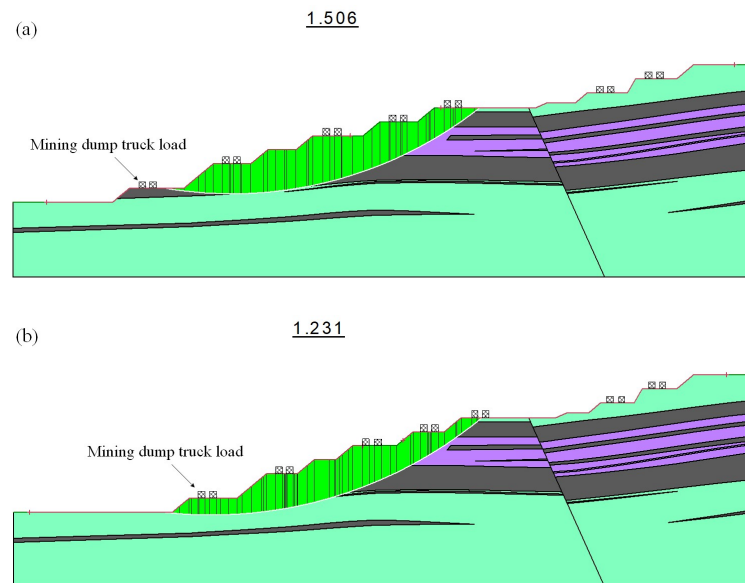


Figure 8. South slope stability analysis: (a) original slope; (b) optimized slope. Green indicates sandstone beds, purple marks mudstone beds, and gray-black indicates coal beds. Green striped half arcs indicate sliding surfaces.

4. Discussion

There are two main contributions in this study compared to what is already known. The first is a methodological contribution, i.e., the road width optimization developed in Section 2.3. The second is an applied contribution; using a specific case of an open-pit mine and based on the methodology presented in this paper, we found that using driverless technology to improve the road width can effectively improve the economics of open-pit mining.

4.1. Driverless Technology

Many scholars have focused on how unmanned vehicles can cause improved transportation efficiency and the establishment of real-time dynamic road networks and other aspects of production and transportation, as well as how unmanned vehicles can avoid obstacles, identify obstacles, undertake emergency braking, and other aspects of safety. Hong et al. found that the optimized scheduling of driverless electric trucks significantly reduces the total energy consumption during terminal operations, outperforming traditional diesel trucks and automated guided vehicles (AGVs) in terms of efficiency, economy, and social benefits [22]. Zhang et al. presented a study on an obstacle avoidance planning method for driverless trackless rubber-tired vehicles (TRTV) in the confined spaces of deep wells [23]. However, nobody has redesigned the road widths for unmanned vehicles. The reason for this is that it would be costly and unnecessary.

This paper has analyzed the differences between manned and unmanned driving, focusing on the construction of open-pit mine transportation roads. It has identified personnel, vehicles, roads, and the environment as the four key factors influencing road construction. In unmanned roads, the personnel factor is eliminated, highlighting the primary difference; the nature of the vehicle in transit changes from driver-operated to system-operated. Consequently, the road and environment remain unchanged. Therefore, our research on unmanned road construction has primarily revolved around studying unmanned vehicles.

4.2. Road Design

This paper has addressed the specific context of a driverless open-pit mine road relating to two main elements—the lane width and the lateral safety distance. In Section 2.1

of this paper, it was mentioned that lane widths need to be referenced to the width of the largest trucks used in an open-pit mine, while safety distances are generally determined empirically by experts. Chang et al. focused on a case study in Beijing. The authors analyzed the relationships between the lane width and various factors, including the saturation flow rate, lateral safety distance, traffic crash rate, and driver comfort, utilizing data from over 3000 existing crossroads and detailed surveys at seven intersections with varying lane widths. The study employed the Delphi method to evaluate the index weights of design-related factors, concluding that the lateral safety distance is the most critical factor in lane width design [24]. Therefore, for lateral safety distances, this paper investigated the differences in lateral deviation distances occurring in manned and driverless trucks based on differences in driver and sensor reaction times and identified the road widths that can be reduced.

According to our research, the lateral safety distance for a truck to travel on a road is determined by objectively assessing the lateral offset distance during travel. The width of a road used for transportation in open-pit mines depends on the truck size, terrain conditions, transport operations, safety, efficiency, and other factors. The optimal road width for safe truck operation requires the careful consideration of various factors. This includes the distance and safety clearance between two passing vehicles, as well as the driver's reaction time and speed. As a result, we derived an equation to estimate the maximum lateral offset distance based on the offset angle and speed at which the truck is travelling. Mecheri et al. investigated how the lane width, shoulder width, and road cross-sectional reallocation affect the driver's lateral positioning, lateral position variability, and driving speed [25]. They found that reductions in lane width caused drivers to drive their vehicles in the center of more advanced roads. However, driverless cars have no such worries.

When discussing road width design, it is important to note that this paper differs from other studies in that optimizing road widths for open-pit mines can be economically beneficial, while optimizing urban road widths can be costly. Chen et al. focused on how the optimal balance between vehicle lane widths and pavement widths on roads in urban areas can minimize the safety and construction costs [26]. The research incorporated both safety costs and agency costs to determine the optimal road space allocation and evaluated how different weightings of these costs impact the optimal allocation of lane and footpath widths. In contrast, roads in open-pit mines are constantly changing and there are many coal resources under such roads. If the road width can be reduced, the coal underneath the road can be recovered, generating economic benefits.

4.3. Limitations and Future Work

In contrast to other studies, our study focused on the reaction time differences between manned and unmanned vehicles when perceiving lateral offsets, without taking into account other factors. Furthermore, this study was biased towards the mechanical analysis of lateral truck deflections and did not include field practice in this area. In the future, when researching the influence of driverless technologies on the building of open-pit mine transportation roads, we could include a mechanical analysis, numerical simulation, field practice, and additional factors.

This study offers technical assistance for building unmanned transportation roads in open-pit mines, demonstrating its practical application and potential economic benefits for constructing intelligent mines in existing sites. Further research is recommended to consider the surface conditions and environmental factors affecting open-pit mine transportation roads.

5. Conclusions

Based on the research, the following conclusions are presented:

- (1) Unmanned vehicles have precise sensing and positioning capabilities, with shorter sensing times and stronger reactive capabilities than human drivers. It is clear that autonomous vehicles can potentially offer a significant advantage over human-driven

vehicles in terms of their capability and efficiency. Analyzing the differences between manned and unmanned roads in open-pit mines, we drew the lateral offset back distance curve for mining dump trucks, using the response times of sensors and drivers as independent variables. This curve showed that the corrective distance for manned driving is greater compared to that of unmanned driving.

- (2) A model for the dynamics of the lateral offset in vehicles was created to examine the lateral forces on a truck during offset steering. By analyzing the Northern Heavy Industries NTE240 self-driving mining dump truck, it was discovered that the road width of the unilateral transport lane of an unmanned vehicle, which can be optimized for reduction, can be calculated as $x_{op} = x'_{max} - x_{max} = 1743$ mm.
- (3) Using the Shengli West No. 1 Open-Pit Mine as a case study, this paper optimized the angle of the south slope and calculated the resulting economic benefits for end-slope mining. This optimization resulted in a stripping volume of 3,273,500 m³, a coal mining volume of 2,496,280 t, and a stripping ratio of 1.31 m³/t. The analysis examined the slope stability of the southern section before and after optimization, along with the impact of truck loading. The slope stability of the slope post-mining was 1.231, satisfying the specifications and confirming the benefits of optimization.

Author Contributions: Conceptualization and methodology, L.H.; writing—original draft preparation, P.L.; writing—review and editing, P.L.; supervision, L.H. All authors have read and agreed to the published version of the manuscript.

Funding: This work was financially supported by the National Natural Science Foundation of China (No. 52374144), Natural Science Foundation of Liaoning Province (CN) (No. 2022-KF-23-10), and Xinjiang Uygur Autonomous Region Science and Technology Major Program (No. 2023A01002).

Institutional Review Board Statement: Not applicable.

Informed Consent Statement: Not applicable.

Data Availability Statement: The raw data supporting the conclusions of this article will be made available by the authors on request.

Conflicts of Interest: The authors do not have any conflict of interest with other entities or researchers.

References

1. Chang, X.; Li, H.; Rong, J.; Chen, X.; Wang, Y. Determining the appropriate lane width at urban signalised intersections—A case study in Beijing. *IET Intell. Transp. Syst.* **2019**, *13*, 1785–1791. [\[CrossRef\]](#)
2. Chen, T.; Sze, N.; Chen, S.; Labi, S. Urban road space allocation incorporating the safety and construction cost impacts of lane and footpath widths. *J. Saf. Res.* **2020**, *75*, 222–232. [\[CrossRef\]](#) [\[PubMed\]](#)
3. Bellamy, D.; Pravica, L. Assessing the impact of driverless haul trucks in Australian surface mining. *Resour. Policy* **2011**, *36*, 149–158. [\[CrossRef\]](#)
4. Kim, D.J.; Bae, J.I.; Lee, K.S.; Lee, D.S.; Leeand, Y.J.; Lee, M.H. Position Recognition System of Autonomous Vehicle via Kalman Filtering. In Proceedings of the Sixteenth International Symposium on Artificial Life and Robotics (AROB 16TH '11), Beppu, Japan, 27–29 January 2011; pp. 834–837.
5. Wang, D.; Zheng, S.; Ren, Y.; Du, D. Path Planning Based on the Improved RRT* Algorithm for the Mining Truck. *CMC-Comput. Mater. Contin.* **2022**, *71*, 3571–3587. [\[CrossRef\]](#)
6. Xiao, D.; Yan, Z.; Li, J.; Gu, Z.; Fu, Y.; Yin, L. Road Extraction From Point Clouds of Open-Pit Mine Using LPFE-Net. *IEEE Geosci. Remote Sens. Lett.* **2023**, *20*, 6501005. [\[CrossRef\]](#)
7. Wang, F.; Zhang, Z. Route Control and Behavior Decision of Intelligent Driverless Truck Based on Artificial Intelligence Technology. *Wirel. Commun. Mob. Comput.* **2022**, *2022*, 7025081. [\[CrossRef\]](#)
8. Ahumada, G.I.; Pintoand, J.D.; Herzog, O. A Dynamic Scheduling Multiagent System for Truck Dispatching in Open-Pit Mines. Agents and Artificial Intelligence, ICAART 2020. In *Proceedings of the 12th International Conference on Agents and Artificial Intelligence (ICAART)*; Rocha, A.P., Steels, L., VanDenHerik, J., Eds.; Springer: Berlin/Heidelberg, Germany, 2021.
9. Postoyev, G.P.; Kazeev, A.I.; Kuchukov, M.M. The Coulomb-Mohr Law and the Change in the Stress-Strain State of a Landslide Prone Mass. *Dokl. Earth Sci.* **2022**, *507* (Suppl. 1), S216–S224. [\[CrossRef\]](#)
10. Liu, H.; Pan, W.; Hu, Y.; Li, C.; Yuan, X.; Long, T. A Detection and Tracking Method Based on Heterogeneous Multi-Sensor Fusion for Unmanned Mining Trucks. *Sensors* **2022**, *22*, 5989. [\[CrossRef\]](#) [\[PubMed\]](#)

11. Hong, C.; Guo, Y.; Wang, Y.; Li, T. The integrated scheduling optimization for container handling by using driverless electric truck in automated container terminal. *Sustainability* **2023**, *15*, 5536. [[CrossRef](#)]
12. Yu, J.J.Q. Two-Stage Request Scheduling for Autonomous Vehicle Logistic System. *IEEE Trans. Intell. Transp. Syst.* **2019**, *20*, 1917–1929. [[CrossRef](#)]
13. Zamora-Cadenas, L.; Velez, I.; Sierra-Garcia, J.E. UWB-Based Safety System for Autonomous Guided Vehicles without Hardware on the Infrastructure. *IEEE Access* **2021**, *9*, 96430–96443. [[CrossRef](#)]
14. Mecheri, S.; Rosey, F.; Lobjois, R. The effects of lane width, shoulder width, and road cross-sectional reallocation on drivers' behavioral adaptations. *Accid. Anal. Prev.* **2017**, *104*, 65–73. [[CrossRef](#)] [[PubMed](#)]
15. Wang, P.K.; Torriente, P.A.; Collinsand, L.M.; Morton, K.D. Rapid Position Estimation and Tracking for Autonomous Driving. Unmanned systems technology XIV. In *Proceedings of the Conference on Unmanned Systems Technology XIV*; Karlsen, R.E., Gage, D.W., Shoemaker, C.M., Gerhart, G.R., Eds.; SPIE: Baltimore, MD, USA, 2012.
16. Liu, Q.; Li, X.; Yuan, S.; Li, Z. Decision-Making Technology for Autonomous Vehicles: Learning-Based Methods, Applications and Future Outlook. In *Proceedings of the 2021 IEEE Intelligent Transportation Systems Conference (ITSC)*, Indianapolis, IN, USA, 19–22 September 2021.
17. Zheng, R.; Nakano, K.; Yamabe, S.; Aki, M.; Nakamura, H.; Suda, Y. Study on Emergency-Avoidance Braking for the Automatic Platooning of Trucks. *IEEE Trans. Intell. Transp. Syst.* **2014**, *15*, 1748–1757. [[CrossRef](#)]
18. Shukla, S.; Kasarapu, S.; Hasan, R.; Manoj, P.D.S.; Shen, H.Y.; IEEE. UBOL: User-Behavior-Aware One-Shot Learning for Safe Autonomous Driving. In *Proceedings of the 2022 Fifth International Conference on Connected and Autonomous Driving (MetroCAD 2022)*, Detroit, MI, USA, 28–29 April 2022.
19. Zhang, S.; Lu, C.; Jiang, S.; Shan, L.; Xiong, N.N. An Unmanned Intelligent Transportation Scheduling System for Open-Pit Mine Vehicles Based on 5G and Big Data. *IEEE Access* **2020**, *8*, 135524–135539. [[CrossRef](#)]
20. Tannant, D.; Regensburg, B. *Guidelines for Mine Haul Road Design*; University of British Columbia Library: Vancouver, BC, Canada, 2010; pp. 1–111.
21. Zhang, D.M.; Yin, G.Z.; Chen, J.A.; Dai, G.F. Stability Analysis of Multi-step Anti-tilt Slope at Open-pit Mine. *Disaster Adv.* **2010**, *3*, 30–34.
22. Yang, W.; Yang, J.; Liang, J.; Zhang, N. Implementation of velocity optimisation strategy based on preview road information to trade off transport time and fuel consumption for hybrid mining trucks. *IET Intell. Transp. Syst.* **2019**, *13*, 194–200. [[CrossRef](#)]
23. Wo, X.; Li, G.; Sun, Y.; Li, J.; Yang, S.; Hao, H. The Changing Tendency and Association Analysis of Intelligent Coal Mines in China: A Policy Text Mining Study. *Sustainability* **2022**, *14*, 11650. [[CrossRef](#)]
24. Xu, X.; Wang, Z.; Huang, P.; Tian, S.; Bi, L. Open-Pit Map: An HD Map Data Model for Open-Pit Mines. *Appl. Sci.* **2023**, *13*, 12681. [[CrossRef](#)]
25. Guo, Z.; Liu, F.; Shang, Y.; Li, Z.; Qin, P. Longitudinal and lateral stability control for autonomous vehicles in curved road scenarios with road undulation. *Eng. Comput.* **2023**, *40*, 2814–2840. [[CrossRef](#)]
26. Zhang, X.; Yang, C.; Gu, Z.; Tang, C.; Zhu, Z.; Zhang, Y.; Qian, J.; Li, X. Obstacle avoidance for trackless rubber-tired vehicle based on risk-grid particle swarm optimization in confined space of deep well. *IEEE Trans. Veh. Technol.* **2023**, *72*, 11291–11303. [[CrossRef](#)]

Disclaimer/Publisher's Note: The statements, opinions and data contained in all publications are solely those of the individual author(s) and contributor(s) and not of MDPI and/or the editor(s). MDPI and/or the editor(s) disclaim responsibility for any injury to people or property resulting from any ideas, methods, instructions or products referred to in the content.